Published in Australian Journal of Chemistry 63, issue 11, 1529-1537, 2010
which should be used for any reference to this work

Synthesis, Characterization and Anticancer Activity of Porphyrin-Containing Organometallic Cubes

Nicolas P. E. Barry,[A] *Olivier Zava,*[B] *Paul J. Dyson,*[B] *and Bruno Therrien*[A,C]

[A]Institute of Chemistry, University of Neuchatel, 51 Avenue de Bellevaux, CH-2000 Neuchatel, Switzerland.
[B]Institut des Sciences et Ingénierie Chimique, Ecole Polytechnique Fédérale de Lausanne (EPFL), CH-1015 Lausanne, Switzerland.
[C]Corresponding author. Email: bruno.therrien@unine.ch

Self-assembly of 5,10,15,20-tetra(4-pyridyl)porphyrin (tpp-H_2) and 5,10,15,20-tetra(4-pyridyl)porphyrin-M(II) (M = Ni (tpp-Ni); Zn (tpp-Zn)) tetradentate panels with the dinuclear *p*-cymene ruthenium clips $[Ru_2(p\text{-cymene})_2(C_2O_4)Cl_2]$ and $[Ru_2(p\text{-cymene})_2(C_6H_2O_4)Cl_2]$ (C_2O_4 = oxalato; $C_6H_2O_4$ = 2,5-dioxydo-1,4-benzoquinonato) affords the cationic organometallic cubes: $[Ru_8(p\text{-cymene})_8(\text{tpp-}H_2)_2(C_2O_4)_4]^{8+}$ (**1**); $[Ru_8(p\text{-cymene})_8(\text{tpp-Ni})_2(C_2O_4)_4]^{8+}$ (**2**); $[Ru_8(p\text{-cymene})_8(\text{tpp-Zn})_2(C_2O_4)_4]^{8+}$ (**3**); $[Ru_8(p\text{-cymene})_8(\text{tpp-}H_2)_2(C_6H_2O_4)_4]^{8+}$ (**4**); $[Ru_8(p\text{-cymene})_8(\text{tpp-Ni})_2(C_6H_2O_4)_4]^{8+}$ (**5**); and $[Ru_8(p\text{-cymene})_8(\text{tpp-Zn})_2(C_6H_2O_4)_4]^{8+}$ (**6**). In addition, the new dinuclear arene ruthenium 2,5-dioxydo-1,4-benzoquinonato clips $[Ru_2(\text{indane})_2(C_6H_2O_4)Cl_2]$ (**7**) and $[Ru_2(\text{nonylbenzene})_2(C_6H_2O_4)Cl_2]$ (**8**) react in methanol with tpp-H_2 in the presence of silver triflate to afford the corresponding cationic cubes $[Ru_8(\text{indane})_8(\text{tpp-}H_2)_2(C_6H_2O_4)_4]^{8+}$ (**9**) and $[Ru_8(\text{nonylbenzene})_8(\text{tpp-}H_2)_2(C_6H_2O_4)_4]^{8+}$ (**10**) respectively. All cationic metalla-cubes were isolated as triflate salts and characterized by NMR, infrared, electro-spray mass spectrometry and UV-visible spectroscopy. Moreover, the formation of unsymmetrical metalla-cubes built using a mixture of the different porphyrin panels during the self-assembly of the 2,5-dioxydo-1,4-benzoquinonato metalla-cubes, $[Ru_8(p\text{-cymene})_8(\text{tpp-}H_2)(\text{tpp-Ni})(C_6H_2O_4)_4]^{8+}$ (**11**), $[Ru_8(p\text{-cymene})_8(\text{tpp-}H_2)(\text{tpp-Zn})(C_6H_2O_4)_4]^{8+}$ (**12**), and $[Ru_8(p\text{-cymene})_8(\text{tpp-Ni})(\text{tpp-Zn})(C_6H_2O_4)_4]^{8+}$ (**13**), was studied by electro-spray mass spectrometry. The cytotoxicities of all metalla-cubes as well as the mixtures containing the unsymmetrical metalla-cubes were established on human ovarian A2780 and A2780cisR cancer cell lines. All symmetrical compounds are equally cytotoxic (IC_{50} = 7–15 μM) (IC_{50} being the drug concentration necessary for 50% inhibition of cell viability) against both A2780 and cisplatin-resistant A2780cisR cancer cells, with stronger cytotoxicities (IC_{50} = 2–5 μM) observed for the mixtures containing the unsymmetrical 2,5-dioxydo-1,4-benzoquinonato metalla-cubes.

Introduction

Most solid tumours possess a unique extracellular environment comprising a hypervasculature, a defective vascular architecture, and impaired lymphatic drainage.[1] The resulting enhanced vascular permeability of solid tumours has became an effective way to target cancer cells.[2] Whereas the normal endothelial layer surrounding the blood vessels feeding healthy cells restricts the size of molecules that can diffuse from the blood, the endothelial layer of blood vessels in diseased tissues is more porous towards large molecules, providing access to the surrounding cancer cells. Moreover, diseased tissue does not usually have a lymphatic drainage system, so once large molecules have entered the tumour environment, they are more likely to be retained. This passive targeting of tumours by large molecules is referred to as the 'enhanced permeability and retention' (EPR) effect.[3]

Owing to the clinical success of platinum-based cancer drugs,[4] macromolecular derivatives have been evaluated in an attempt to target tumours more effectively to reduce the severe toxic side effects and to overcome resistance associated with platinum agents.[5] In recent years, ruthenium compounds have been shown to exhibit promising anticancer activity,[6] with two compounds being evaluated in clinical trials.[7] Ruthenium complexes are believed to bind with large biomolecules[8] in the plasma and consequently could take advantage of the EPR effect. However, larger multinuclear ruthenium complexes could potentially use the EPR effect without having to bind to biomolecules.

There has been increasing interest in the anticancer properties of arene ruthenium (organometallic) compounds,[9] and very recently, we found that rectangular tetranuclear arene ruthenium complex cations incorporating 2,5-dioxydo-1,4-benzoquinato ($C_6H_2O_4$) and dipyridyl linkers were cytotoxic against human ovarian (A2780) cancer cells and showed a pronounced size effect,[10] as was observed by others[11] for polynuclear compounds. While the smaller rectangles containing 4,4′-bipyridine (bipy) bridges, $[Ru_4(p\text{-cymene})_4(\text{bipy})_2(C_6H_2O_4)_2]^{4+}$ and $[Ru_4(\text{hexamethylbenzene})_4(\text{bipy})_2$

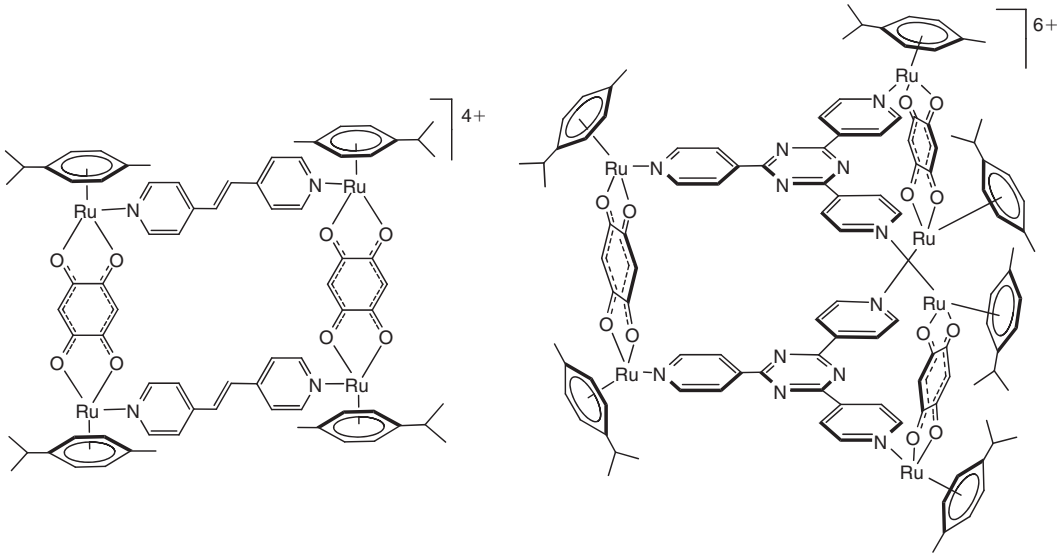

Tetranuclear arene ruthenium complex

Hexanuclear arene ruthenium complex

Chart 1.

$(C_6H_2O_4)_2]^{4+}$ are only moderately cytotoxic ($IC_{50} = 66$ and 27 μM respectively) (IC_{50} being the drug concentration necessary for 50% inhibition of cell viability), the larger rectangles containing 1,2-bis(4-pyridyl)ethene (bpe) bridges, $[Ru_4(p\text{-cymene})_4(bpe)_2(C_6H_2O_4)_2]^{4+}$ (Chart 1) and $[Ru_4(hexamethylbenzene)_4(bpe)_2(C_6H_2O_4)_2]^{4+}$ show good cytotoxicities ($IC_{50} = 6$ and 4 μM respectively). We also prepared hexanuclear arene ruthenium complexes that form hexacationic cages using 2,5-dioxydo-1,4-benzoquinato bridges and tridentate 2,4,6-tris (4-pyridyl)1,3,5-triazine (tpt) panels, which are active against human ovarian (A2780) cancer cells (Chart 1). The empty hexaruthenium cage already possesses an IC_{50} value of 23 μM; using the platinum-containing cage, the cytotoxicity doubles ($IC_{50} = 12$ μM), and using the palladium-containing cage, the activity goes up by a factor of 20 ($IC_{50} = 1$ μM), whereas free $Pt(acac)_2$ and $Pd(acac)_2$ (acac = acetylacetonato) are completely inactive owing to their insolubility in water.[12] Direct evidence of this 'Trojan Horse' strategy to selectively deliver and release a hydrophobic-containing host to cancer cells was obtained using a fluorescent molecule as a cargo.[13]

We have now extended this strategy and synthesized larger metalla-assemblies incorporating tetrapyridyl-porphyrin panels, 5,10,15,20-tetra(4-pyridyl)porphyrin (tpp-H_2) and 5,10,15,20-tetra(4-pyridyl)porphyrin-M(II) (M = Ni (tpp-Ni), Zn (tpp-Zn)), connected by dinuclear arene ruthenium clips $[Ru_2(p\text{-cymene})_2(C_2O_4)Cl_2]$, $[Ru_2(p\text{-cymene})_2(C_6H_2O_4)Cl_2]$, $[Ru_2(indane)_2(C_6H_2O_4)Cl_2]$, and $[Ru_2(nonylbenzene)_2(C_6H_2O_4)Cl_2]$ (C_2O_4 = oxalato; $C_6H_2O_4$ = 2,5-dioxydo-1,4-benzoquinonato = dobq). We have also studied the formation of unsymmetrical metalla-cubes constructed from mixtures of different porphyrin panels during the synthesis of the cubes. All these octacationic metalla-cubes have been characterized and evaluated in vitro against human ovarian cancer cell lines.

Results and Discussion

Syntheses, Solubility, and Stability

As shown previously, the synthesis of arene ruthenium metalla-cubes [**1**],[14] [**3**],[15] [**4**],[16] and [**6**][15] is straightforward. Accordingly, for the nickel porphyrin derivatives $[Ru_8(p\text{-cymene})_8(tpp\text{-}Ni)_2(C_2O_4)_4]^{8+}$ (**2**) and $[Ru_8(p\text{-cymene})_8(tpp\text{-}Ni)_2(C_6H_2O_4)_4]^{8+}$ (**5**), the addition of silver triflate to the dinuclear metalla-clips $[Ru_2(p\text{-cymene})_2(C_2O_4)Cl_2]$ and $[Ru_2(p\text{-cymene})_2(C_6H_2O_4)Cl_2]$, in the presence of 5,10,15,20-tetra(4-pyridyl)porphyrin-Ni(II) (tpp-Ni) leads in good yield to the formation of **2** and **5**. The *p*-cymene ruthenium metalla-cubes **1**–**6** are presented in Fig. 1.

Following the same two-step strategy in which the new dinuclear complexes $[Ru_2(indane)_2(C_6H_2O_4)Cl_2]$ and $[Ru_2(nonylbenzene)_2(C_6H_2O_4)Cl_2]$ are used as metalla-clips, the metalla-cubes $[Ru_8(indane)_8(tpp\text{-}H_2)_2(C_6H_2O_4)_4]^{8+}$ ([**9**]) and $[Ru_8(nonylbenzene)_8(tpp\text{-}H_2)_2(C_6H_2O_4)_4]^{8+}$ ([**10**]) were prepared (Scheme 1), isolated as their triflate salts and characterized by IR, NMR, electrospray ionization mass spectrometry (ESI-MS) and by elemental analysis (see below and Experimental). The metalla-cubes are quite soluble in dichloromethane, acetonitrile, acetone, and DMSO but poorly soluble in methanol and water. The stability of the metalla-cubes in D_2O was monitored by ^1H NMR spectroscopy, and following 48 h of heating at 60°C, no degradation was observed.

Characterization

The ^1H NMR spectra (in CD_3CN or CD_2Cl_2) of **2**, **5**, **9**, and **10**, the new metalla-cubes described herein, display a similar signal pattern to the corresponding porphyrin (tpp-H_2 or tpp-Ni) and arene protons. In the case of metalla-cubes **2** and **5** (arene = *p*-cymene), four doublets are observed in the region 6.2–5.9 ppm for the arene protons, whereas in **9** (arene = indane), two doublets and two triplets and in **10** (arene = nonylbenzene), one doublet of doublets, two doublets and one triplet are observed in the same region. In **9** and **10**, an additional signal at $\delta \sim -6.96$ ppm corresponding to the N–H protons of the tpp-H_2 porphyrin panels is observed, whereas in **5**, **9**, and **10**, the benzoquinonato singlet is observed at ~6.2 ppm. Moreover, the tpp panels give between 9.5 and 7.0 ppm a total of six multiplets corresponding to four pyridyl and two pyrrole protons. The non-equivalence of the *endo* (pointing inwards) and *exo* (pointing outwards) pyridyl protons is not surprising; a similar signal pattern has been observed with the known

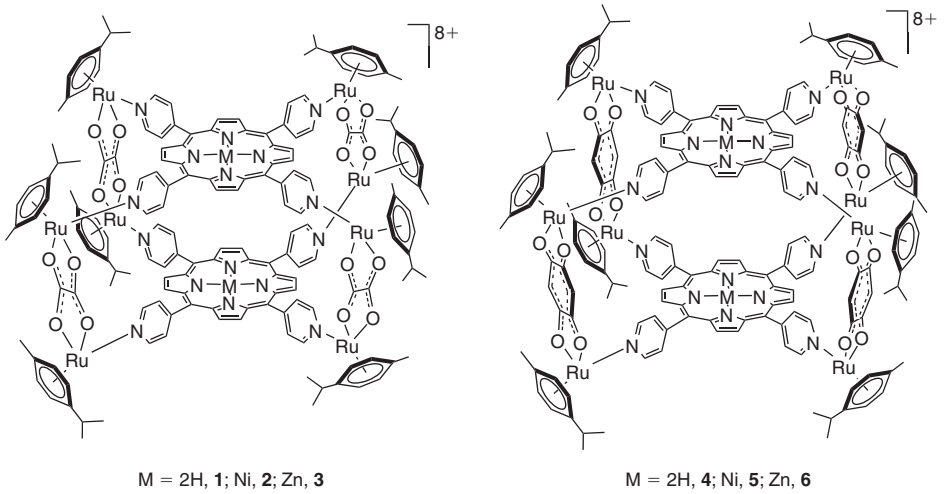

Fig. 1. Metalla-cubes **1**–**6**.

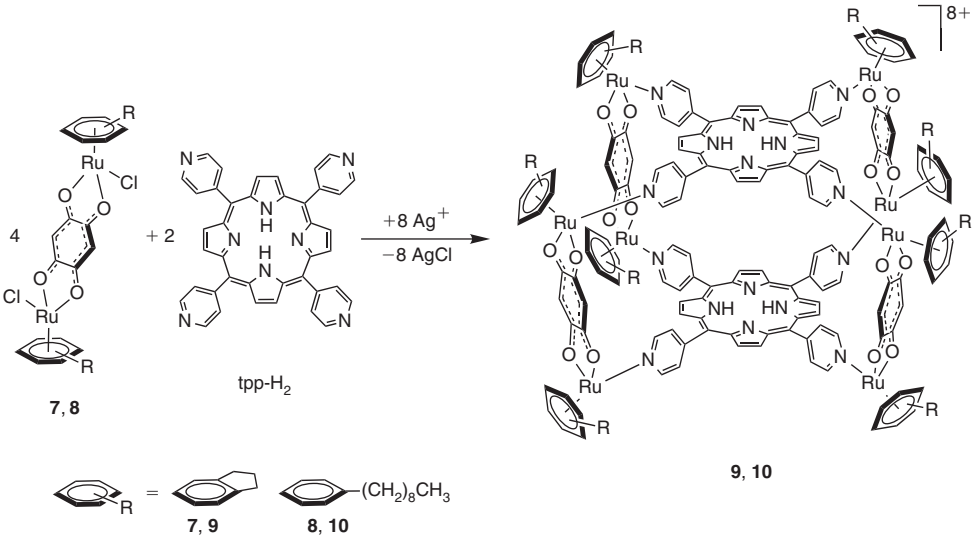

Scheme 1. Synthesis of metalla-cubes **9** and **10** from metalla-clips **7** and **8**.

metalla-cubes **1**, **3**, **4**, and **6**,[15] and is consistent with previous observations in related metalla-prisms,[17] with the presence of diastereotopic protons being attributed to a tilt of the dinuclear metalla-clips and a twist of the two porphyrins panels, thus leading to helical chirality (Fig. 2).

The IR spectra of **2**, **5**, **9**, and **10**, as well as the already reported metalla-cubes **1**, **3**, **4**, and **6**, are dominated by absorptions of the coordinated porphyrin panels with, in particular, a strong in-plane N–H deformation at ~1220 cm^{-1} observed in **1**, **4**, **9**, and **10**,[18] and the bands assigned to the C=C and C=N skeletal modes of the porphyrins located between 1620 and 1400 cm^{-1}.[19] Moreover, the bands associated with the *OO*∩*OO* bridges, including the strong C=O stretching vibration (at ~1530 cm^{-1}), are only slightly shifted compared with the corresponding vibrations observed in the dinuclear complexes $[Ru_2(p\text{-cymene})_2(C_2O_4)Cl_2]$[20] and $[Ru_2(arene)_2(C_6H_2O_4)Cl_2]$.[12] In addition to the porphyrin and *OO*∩*OO* absorptions, strong stretching vibrations due to the triflate anions (1260(s), 1030(s), 638(m) cm^{-1}) are also observed in the IR spectra of the salts **[1–6]**$[CF_3SO_3]_8$ and **[9–10]**$[CF_3SO_3]_8$.

Under the conditions of ESI-MS, all the metalla-cubes **1**–**6**, **9**, and **10** are remarkably stable. The ESI-MS spectra of **2**, **5**, **9**, and **10** show peaks corresponding to $[\mathbf{2} + (CF_3SO_3)_4]^{4+}$, $[\mathbf{5} + (CF_3SO_3)_4]^{4+}$, $[\mathbf{9} + (CF_3SO_3)_4]^{4+}$, and $[\mathbf{10} + (CF_3SO_3)_4]^{4+}$, at *m*/*z* 1045.0, 1095.5, 1035.5, and 1207.8 respectively, which are assigned unambiguously on the basis of their characteristic Ru_8 isotope patterns. Fig. 3 shows the ESI-MS spectrum of $[\mathbf{9}][CF_3SO_3]_8$ in acetonitrile.

Electronic absorption spectra of **2**, **5**, **9**, and **10** as well as the porphyrin panels (tpp-H_2 and tpp-Ni) were acquired in dichloromethane at 10^{-5} M concentration in the range 250–800 nm (Fig. 4). The UV-visible spectra of all compounds are characterized by intense absorptions due to the porphyrin panels, including the Soret band at ~400 nm and a series of Q bands between 500 and 700 nm. In all complexes, compared with the free porphyrins, the Soret band is blue-shifted and the full width at half-maximum ($\Delta\nu$) increased. In the case of metalla-cube **9**, the full width at half-maximum ($\Delta\nu = 1471\ cm^{-1}$) is 33% larger than the width of tpp-H_2 (1106 cm^{-1}). In all metalla-cubes, a weak hypsochromic shift of the Soret band and a strong

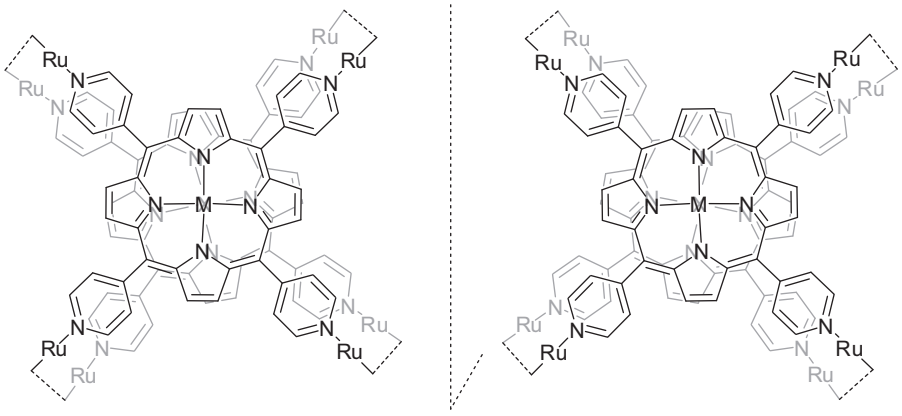

Fig. 2. Chiral conformation of metalla-cubes **1**–**6**, **9**, and **10**.

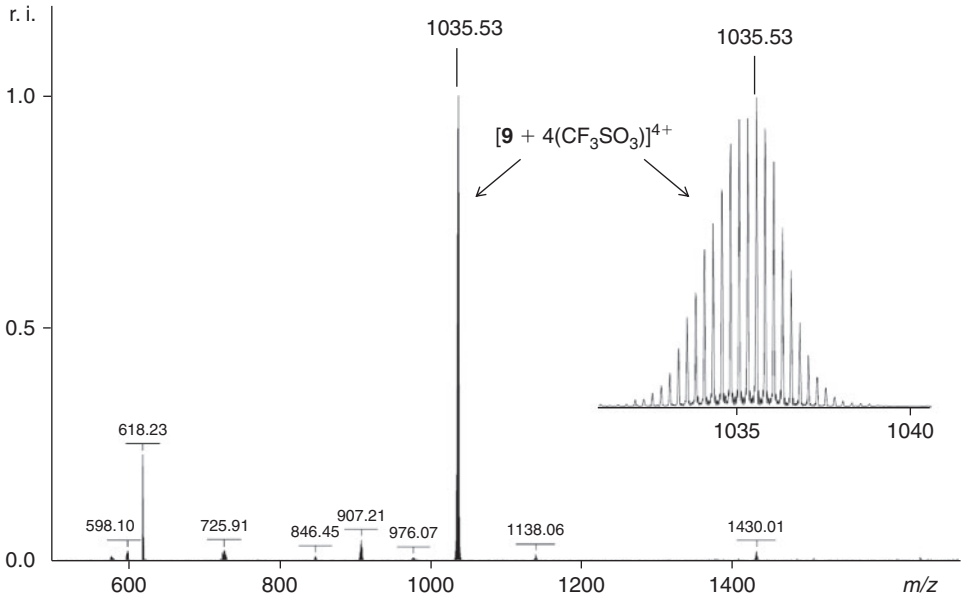

Fig. 3. Electrospray ionization mass spectrometry (ESI-MS) of [**9**][CF_3SO_3]$_8$.

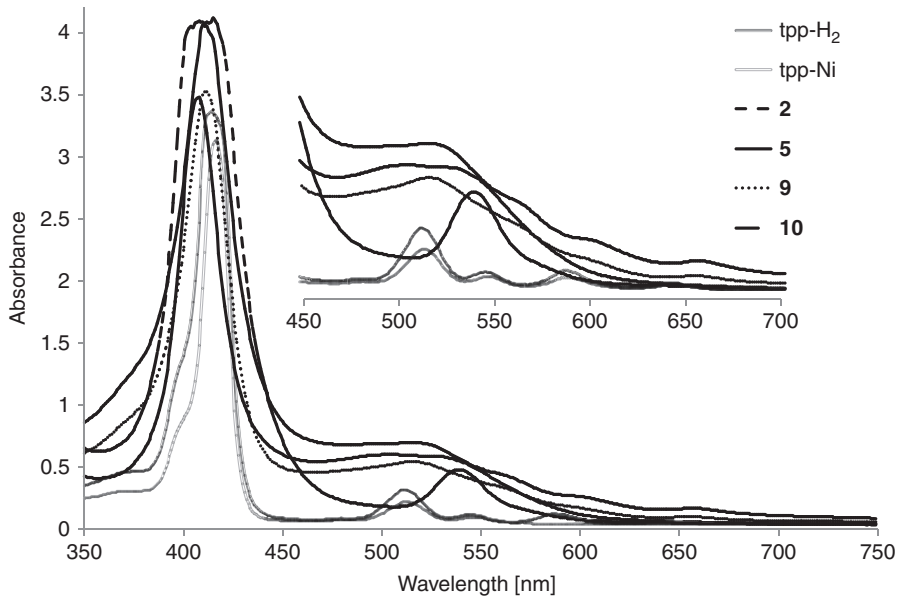

Fig. 4. UV-visible spectra of tpp-H_2, tpp-Ni, and metalla-cubes **2**, **5**, **9**, and **10** in dichloromethane (10^{-5} M).

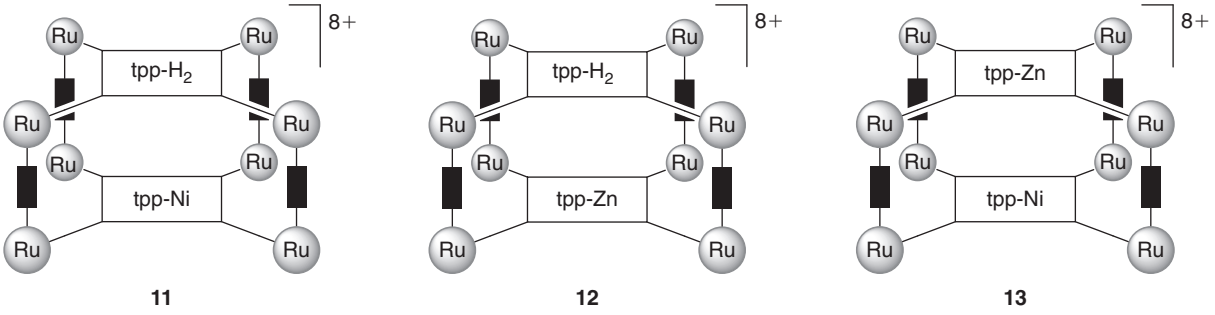

Fig. 5. The unsymmetrical metalla-cubes **11**–**13**.

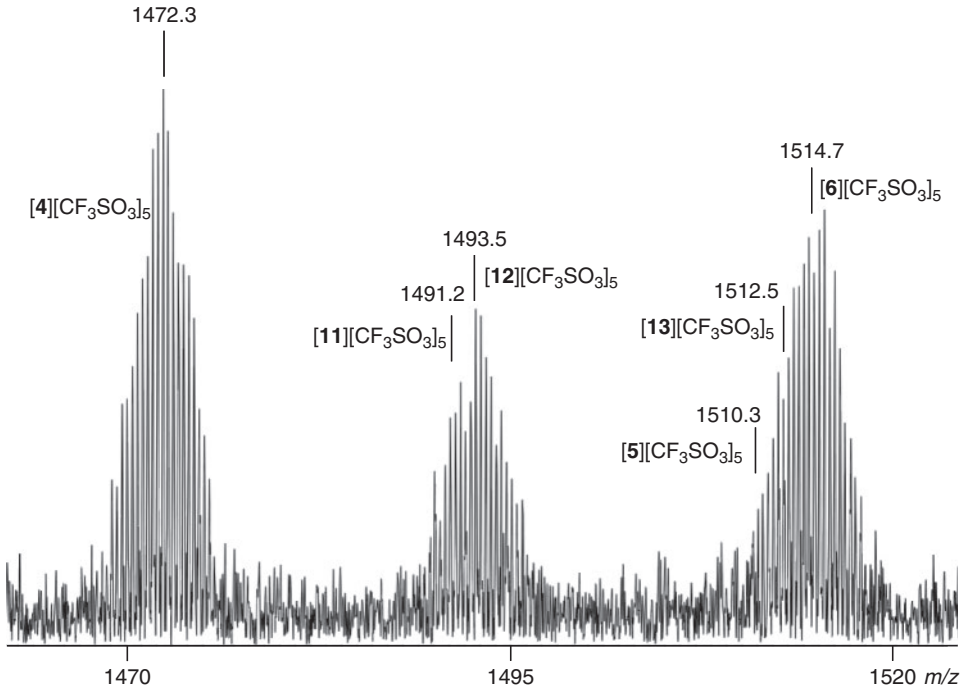

Fig. 6. Electrospray ionization mass spectrometry (ESI-MS) of Mx_4 showing the presence of **4**, **5**, **6**, **11**, **12**, and **13**.

bathochromic shift of the Q bands are observed with respect to the free porphyrins. These photophysical changes in the UV-visible spectra of the metalla-cubes are characteristic of sandwich-type porphyrin dimers.[21]

Unsymmetrical Metalla-Cubes

As mentioned above, metalla-cubes **1**–**6**, **9**, and **10** are particularly stable under the conditions of ESI-MS. For this reason, we used this technique to investigate the formation of unsymmetrical metalla-cubes, i.e. the formation of metalla-cubes built from two different porphyrin panels. Consequently, a stock solution of the dinuclear metalla-clip $[Ru_2(p\text{-cymene})_2(C_6H_2O_4)Cl_2]$ with silver triflate was freshly prepared in methanol. Next, mixtures containing equimolar amount of porphyrin panels (Mx_1: tpp-H_2 + tpp-Ni; Mx_2: tpp-H_2 + tpp-Zn; Mx_3: tpp-Ni + tpp-Zn; Mx_4: tpp-H_2 + tpp-Ni + tpp-Zn) were added to four fractions of the stock solution and heated at reflux for 48 h, leading to the formation of mixtures of symmetrical and unsymmetrical metalla-cubes (in Mx_1: **4** + **5** + **11**; Mx_2: **4** + **6** + **12**; Mx_3: **5** + **6** + **13**; Mx_4: **4** + **5** + **6** + **11** + **12** + **13**) as determined by ^{1}H NMR spectroscopy. The precipitates obtained were directly analysed by ESI-MS without further purification or separation. All attempts to separate the metalla-cubes were unsuccessful. The proposed structures of the unsymmetrical metalla-cubes **11**, **12**, and **13** are presented in Fig. 5.

The ESI-MS spectrum of a solution of Mx_1 shows the formation of the expected metalla-cubes **4** and **5** as well as the formation of the unsymmetrical metalla-cube $[Ru_8(p\text{-cymene})_8(tpp\text{-}H_2)(tpp\text{-Ni})(C_6H_2O_4)_4]^{8+}$ (**11**). In the same way, the formation of $[Ru_8(p\text{-cymene})_8(tpp\text{-}H_2)(tpp\text{-Zn})(C_6H_2O_4)_4]^{8+}$ (**12**) and $[Ru_8(p\text{-cymene})_8(tpp\text{-Ni})(tpp\text{-Zn})(C_6H_2O_4)_4]^{8+}$ (**13**) is observed in mixtures Mx_2 and Mx_3 respectively. Finally, in Mx_4, the formation of all unsymmetrical and symmetrical metalla-cubes can be observed by ESI-MS (Fig. 6). This study confirms that the formation of metalla-cubes with two different porphyrin panels is possible.

Antiproliferative Activity

The antiproliferative activity of the isolated metalla-cubes **1**–**6**, **9**, **10**, the stoichiometric mixtures of metalla-cubes **4**–**6** (Table 1,

Table 1. IC_{50}[A] values with standard deviations of complexes 1–6, 9, 10, Mx_1–Mx_4 and stoichiometric mixtures of 4–6 in A2780 and A2780cisR cell lines

Entry	Compounds	IC_{50} A2780 [μM]	IC_{50} A2780cisR [μM]
1	**1**	57.6 ± 1.9	44.2 ± 5.6
2	**2**	41.5 ± 5.8	49.5 ± 8.9
3	**3**	34.5 ± 7.5	35.7 ± 8.0
4	**4**	8.0 ± 4.5	7.0 ± 4.5
5	**5**	15.5 ± 4.5	14.8 ± 4.5
6	**6**	7.6 ± 0.6	9.8 ± 0.4
7	**9**	19.4 ± 4.5	21.5 ± 3.8
8	**10**	21.2 ± 2.5	24.1 ± 5.2
9	Mx_1 (**4** + **5** + **11**)	3.3 ± 1.1	2.2 ± 0.9
10	Mx_2 (**4** + **6** + **12**)	2.8 ± 0.1	2.0 ± 0.5
11	Mx_3 (**5** + **6** + **13**)	5.4 ± 1.3	4.3 ± 0.3
12	Mx_4 (**4** + **5** + **6** + **11** + **12** + **13**)	3.2 ± 0.4	2.5 ± 0.3
13	**4** + **5**	14 ± 3.9	16.2 ± 5.0
14	**4** + **6**	7.1 ± 1.5	9.2 ± 0.5
15	**5** + **6**	13.8 ± 5.2	16.4 ± 4.3
16	**4** + **5** + **6**	12.4 ± 1.4	16.5 ± 1.3
17	cisplatin	2.2 ± 0.8	12.2 ± 1.2

[A] IC_{50} is the drug concentration necessary for 50% inhibition of cell viability.

entries 13 to 16) and the mixtures Mx_1–Mx_4 containing the unsymmetrical metalla-cubes (Table 1, entries 9 to 12) were evaluated against the A2780 (cisplatin-sensitive) and A2780cisR (cisplatin-resistant) human ovarian cancer cell lines. Their cytotoxicities, in comparison with cisplatin, are presented in Table 1.

All compounds show similar cytotoxicities towards both cisplatin-sensitive and cisplatin-resistant cancer cell lines, suggesting that they do not share the same mechanisms of action as the reference drug, i.e. cisplatin. Moreover, among the compounds tested, additional trends can be drawn from these results: the oxalato-containing metalla-cubes **1**–**3** are at least an order of magnitude less cytotoxic than the 2,5-dioxydo-1,4-benzoquinonato analogues **4**–**6**, indicating that the nature of the *OO*∩*OO* connecting spacer plays a crucial role. Similarly, the nature of the arene ligand can influence the cytotoxicity of the metalla-cubes. Indeed, the indane and nonylbenzene derivatives, **9** and **10** respectively, are significantly less cytotoxic than the corresponding *p*-cymene analogue **4**. In contrast, metallation of the porphyrin core with the Zn^{2+} ion (metalla-cube **6**) does not modify the activity whereas metallation with Ni^{2+} (metalla-cube **5**) slightly reduces the cytotoxicity of the compound.

Interestingly, the mixtures Mx_1–Mx_4 containing the unsymmetrical metalla-cubes (Table 1, entries 9 to 12) are the most cytotoxic, with activities comparable with cisplatin or superior to cisplatin in the resistant cancer cell line A2780cisR. This distinctive activity is most probably due to the presence of the unsymmetrical metalla-cubes **11**, **12**, and **13** but not due to an additive effect of the metalla-cubes, as the stoichiometric mixtures of the symmetrical metalla-cubes (entries 13 to 16) clearly show, as expected, a cytotoxicity averaging the activity of the parent complexes **4**–**6** (entries 4 to 6). The reason for such a different activity of the unsymmetrical metalla-cubes compared with their symmetrical counterparts is not clear at the moment, but it could be linked to a better internalization of the products, to a different mode of interaction in the cell, or to a greater or lesser overall stability in the cellular environment. Nevertheless, these results are quite unexpected and further studies will be needed to provide an explanation for this difference in cytotoxicity between symmetrical and unsymmetrical metalla-cubes.

Conclusions

A series of octacationic metalla-cubes incorporating porphyrin and metallo-porphyrin panels connected by oxalato and 2,5-dihydroxy-1,4-benzoquinonato arene ruthenium clips have been prepared and characterized by spectroscopic methods. These water-soluble metalla-cubes were screened for in vitro anticancer activity against the A2780 and A2780cisR ovarian cancer cell lines, and the larger assemblies were found to be highly active and equally potent on both cell lines. It is likely that these large complexes would be taken up more efficiently by tumours owing to the EPR effect of cancer cells, thus providing a degree of selectivity and ultimately giving a better efficacy. Further studies are in progress to investigate the surprisingly low IC_{50} values observed for the unsymmetrical metalla-cubes.

Experimental

General

^1H and $^{13}C\{^1H\}$ spectra were recorded on a Bruker AvanceII 400 spectrometer using the residual protonated solvent as internal standard ([D]chloroform: $\delta_H = 7.26$ ppm, [D2]dichloromethane: $\delta_H = 5.32$ ppm, and [D3]acetonitrile: $\delta_H = 1.94$ ppm). Infrared spectra were recorded as KBr pellets on a Perkin–Elmer Fourier-transform (FT)-IR 1720X spectrometer. UV-visible absorption spectra were recorded on an Uvikon 930 spectrophotometer using precision cells made of quartz (1 cm). Microanalyzes were performed by the Laboratory of Pharmaceutical Chemistry, University of Geneva (Switzerland). Electro-spray mass spectra were obtained in positive-ion mode with a Bruker FTMS 4.7-T BioAPEX II mass spectrometer. The dimers $[Ru(p\text{-cymene})Cl_2]_2$[22] and $[Ru(indane)Cl_2]_2$,[23] the dinuclear *p*-cymene ruthenium complexes $[Ru_2(p\text{-cymene})_2$

$(C_2O_4)Cl_2]$,[20] $[Ru_2(p\text{-cymene})_2(C_6H_2O_4)Cl_2]$[12] and the metalla-cubes **1**,[14] **3**,[15] **4**,[16] **6**[15] were prepared according to published methods. $[Ru(nonylbenzene)Cl_2]_2$ was prepared by a Birch-type reduction[24] of the commercially available (Sigma–Aldrich) nonylbenzene. Addition of $RuCl_3 \cdot nH_2O$ in ethanol to the non-isolated 3-nonylcylohexa-1,4-diene using standard reaction and purification conditions afforded the dimer.[25] δ_H (400 MHz, $CDCl_3$, 298 K) 5.66 (dd, ^3J 5.9, ^3J 5.6, 4H, H_{phenyl}), 5.56 (t, 2H, H_{phenyl}), 5.36 (d, 4H, H_{phenyl}), 2.52 (t, ^3J 7.9, 4H, $CH_{2\alpha}$), 1.53 (m, 4H, $CH_{2\beta}$), 1.27 (m, 24H, CH_2), 0.86 (t, ^3J 6.6, 6H, CH_3). $^{13}C\{^1H\}$ NMR (100 MHz, $CDCl_3$, 298 K) 102.8 (C_{phenyl}), 80.4 (CH_{phenyl}), 79.9 (CH_{phenyl}), 78.4 (CH_{phenyl}), 33.8 ($CH_{2\alpha}$), 32.6 ($CH_{2\beta}$), 30.2 (CH_2), 30.1 (CH_2), 30.0 (CH_2), 30.0 (CH_2), 23.4 (CH_2), 14.4 (CH_3). The porphyrin derivatives were commercially available (Sigma–Aldrich, TriPorTech GmbH or Frontier Scientific) and used as received. The other reagents were purchased from Sigma–Aldrich and used as received.

Syntheses

*Metalla-Clips **7** and **8***

A mixture of $[(arene)RuCl_2]_2$ (**7**: indane, 500 mg, 0.86 mmol; **8**: nonylbenzene, 647 mg, 0.86 mmol) and 2,5-dihydroxy-1,4-benzoquinone (120 mg, 0.86 mmol) in ethanol (100 mL) was stirred at reflux for 24 h, then filtered. The black precipitate was washed with cold ethanol, pentane, and dried under vacuum.

7: Yield: 528 mg (95%). ν_{max}/cm^{-1} 3070 (w, aromatic, C–H), 1629 (s, dobq, C=O). λ_{max}/nm ($\varepsilon/M^{-1}\,cm^{-1}$) ($1.0 \times 10^{-5}$ M, CH_2Cl_2) 268 (2.83×10^4). δ_H (400 MHz, $CDCl_3$, 298 K) 6.31 (d, ^3J 7.4, 8H, H_{indane}), 6.22 (d, ^3J 7.3, 8H, H_{indane}), 6.15 (s, 8H, H_q), 6.12 (t, 8H, H_{indane}), 6.05 (t, 8H, H_{indane}), 3.06 (m, 16H, $CH_{2indane}$), 2.95 (m, 8H, $CH_{2indane}$). $^{13}C\{^1H\}$ NMR (100 MHz, $CDCl_3$, 298 K) 184.0 (CO), 104.2 (C_{indane}), 103.7 (C_{indane}), 102.0 (CH_q), 83.0 (CH_{indane}), 82.7 (CH_{indane}), 82.5 (CH_{indane}), 82.4 (CH_{indane}), 30.3 ($CH_{2indane}$), 23.4 ($CH_{2indane}$). Calc. for $C_{24}H_{22}Cl_2O_4Ru_2$ (647.5): C 44.52, H 3.42. Found: C 44.46, H 3.32%.

8: Yield: 690 mg (98%). ν_{max}/cm^{-1} 3068 (w, aromatic, C–H), 1630 (s, dobq, C=O). λ_{max}/nm ($\varepsilon/M^{-1}\,cm^{-1}$) ($1.0 \times 10^{-5}$ M, CH_2Cl_2) 275 (2.81×10^4). δ_H (400 MHz, $CDCl_3$, 298 K) 5.65 (dd, ^3J 5.9, ^3J 5.6, 4H, H_{phenyl}), 5.56 (t, 2H, H_{phenyl}), 5.37 (d, 4H, H_{phenyl}), 2.51 (t, ^3J 7.9, 4H, $CH_{2\alpha}$), 1.53 (m, 4H, $CH_{2\beta}$), 1.27 (m, 24H, CH_2), 0.85 (t, ^3J 6.6, 6H, CH_3). $^{13}C\{^1H\}$ NMR (100 MHz, $CDCl_3$, 298 K) 184.2 (CO), 102.5 (C_{phenyl}), 80.5 (CH_{phenyl}), 79.9 (CH_{phenyl}), 78.4 (CH_{phenyl}), 33.8 ($CH_{2\alpha}$), 32.8 ($CH_{2\beta}$), 30.2 (CH_2), 30.1 (CH_2), 30.0 (CH_2), 29.9 (CH_2), 23.4 (CH_2), 14.5 (CH_3). Calc. for $C_{36}H_{50}Cl_2O_4Ru_2$ (819.8): C 52.74, H 6.15. Found: C 52.66, H 5.97%.

*Metalla-Cubes [**2**][CF_3SO_3]$_8$, [**5**][CF_3SO_3]$_8$, [**9**][CF_3SO_3]$_8$, and [**10**][CF_3SO_3]$_8$*

A mixture of $Ag(CF_3SO_3)$ (165 mg, 0.64 mmol) and $[Ru_2(arene)_2(OO\cap OO)_2Cl_2]$ (0.32 mmol; **2**: *p*-cymene, oxalato, 201 mg; **5**: *p*-cymene, dobq, 218 mg; **9**: indane, dobq, 207 mg; **10**: nonylbenzene, dobq, 262 mg) in methanol (30 mL) was stirred at room temperature for 3 h, then filtered. To the red filtrate, the corresponding porphyrin (0.16 mmol; **2** and **5**: tpp-Ni, 108 mg; **9** and **10**: tpp-H_2, 99 mg) was added. The solution was refluxed for 48 h, and the solvent removed under vacuum. The residue was dissolved in dichloromethane (**2**, **5**, **10**) or acetonitrile (**9**) (3 mL), and diethyl ether added to precipitate the purple (**2** and **5**) or black (**9** and **10**) solid.

[**2**][CF_3SO_3]$_8$: Yield: 305 mg (79%). ν_{max}/cm^{-1} 3069 (m, aromatic, C–H), 1521 (s, oxalato, C=O), 1258 (s, triflate, C–F). λ_{max}/nm ($\varepsilon/M^{-1}\,cm^{-1}$) ($1.0 \times 10^{-5}$ M, CH_2Cl_2) 416 (4.09×10^5), 542 (0.47×10^5). δ_H (400 MHz, CD_2Cl_2, 298 K) 9.25 (d, ^3J 6.3, 8H, H_{pyr}), 9.18 (d, ^3J 7.1, 8H, H'_α), 8.92 (d, ^3J 7.3, 8H, H_β), 8.17 (d, 8H, H_α), 8.10 (d, 8H, H'_{pyr}), 7.91 (d, 8H, H'_β), 6.15 (m, 16H, $H_{p\text{-cym}}$), 5.97 (m, 16H, $H_{p\text{-cym}}$), 3.05 (sept, ^3J 6.8, 4H, $CH(CH_3)_2$), 2.45 (s, 12H, CH_3), 1.49 (d, 24H, $CH(CH_3)_2$). $^{13}C\{^1H\}$ NMR (100 MHz, CD_3CN, 298 K) 172.3 (CO), 153.7 (CH'_α), 151.2 (CH_α), 149.4 ($C_{pyridyl}$), 140.1 (C_{pyr}), 139.9 (C_{pyr}), 133.5 (CH'_β), 133.1 (CH_β), 130.0 (CH'_{pyr}), 129.6 (CH'_{pyr}), 104.2 ($C_{p\text{-cym}}$), 101.3 ($C_{p\text{-cym}}$), 84.2 ($CH_{p\text{-cym}}$), 83.8 ($CH_{p\text{-cym}}$), 83.0 ($CH_{p\text{-cym}}$), 82.6 ($CH_{p\text{-cym}}$), 32.0 ($CH(CH_3)_2$), 21.8 ($CH(CH_3)_2$), 21.2 ($CH(CH_3)_2$), 17.5 (CH_3). *m/z* (ESI) 1045.0 $[\mathbf{2} + (CF_3SO_3)_4]^{4+}$. Calc. for $C_{176}H_{160}F_{24}N_{16}Ni_2O_{40}Ru_8S_8$ (4777.7): C 44.24, H 3.37, N 4.69. Found: C 44.01, H 3.29, N 4.34%.

[**5**][CF_3SO_3]$_8$: Yield: 311 mg (78%). ν_{max}/cm^{-1} 3068 (m, aromatic, C–H), 1520 (s, dobq, C=O), 1258 (s, triflate, C–F). λ_{max}/nm ($\varepsilon/M^{-1}\,cm^{-1}$) ($1.0 \times 10^{-5}$ M, CH_2Cl_2) 409 (3.45×10^5), 533 (0.58×10^5). δ_H (400 MHz, CD_3CN, 298 K) 8.80 (d, ^3J 6.5, 8H, H_{pyr}), 8.77 (d, ^3J 7.2, 8H, H'_α), 8.44 (d, ^3J 7.1, 8H, H_β), 8.32 (d, 8H, H_α), 8.14 (d, 8H, H'_{pyr}), 7.39 (d, 8H, H'_β), 6.19 (d, ^3J 5.7, 8H, $H_{p\text{-cym}}$), 6.15 (d, ^3J 5.6, 8H, $H_{p\text{-cym}}$), 6.11 (s, 8H, H_q), 6.01 (d, 8H, $H_{p\text{-cym}}$), 5.98 (d, 8H, $H_{p\text{-cym}}$), 3.10 (sept, ^3J 6.6, 8H, $CH(CH_3)_2$), 2.42 (s, 24H, CH_3), 1.52 (m, 48H, $CH(CH_3)_2$). $^{13}C\{^1H\}$ NMR (100 MHz, CD_3CN, 298 K) 184.1 (CO), 183.6 (CO), 152.5 (CH'_α), 150.6 (CH_α), 150.5 ($C_{pyridyl}$), 141.1 (C_{pyr}), 140.8 (C_{pyr}), 132.5 (CH'_β), 132.0 (CH_β), 131.2 (CH'_{pyr}), 130.6 (CH'_{pyr}), 104.0 ($C_{p\text{-cym}}$), 101.9 ($C_{p\text{-cym}}$), 98.6 (CH_q), 83.8 ($CH_{p\text{-cym}}$), 83.2 ($CH_{p\text{-cym}}$), 82.5 ($CH_{p\text{-cym}}$), 82.3 ($CH_{p\text{-cym}}$), 31.4 ($CH(CH_3)_2$), 21.9 ($CH(CH_3)_2$), 21.4 ($CH(CH_3)_2$), 17.5 (CH_3). *m/z* (ESI) 1095.5 $[\mathbf{5} + (CF_3SO_3)_4]^{4+}$, 1510.3 $[\mathbf{5} + (CF_3SO_3)_5]^{3+}$. Calc. for $C_{192}H_{168}F_{24}N_{16}Ni_2O_{40}Ru_8S_8$ (4977.9): C 46.33, H 3.40, N 4.50. Found: C 46.08, H 3.28, N 4.41%.

[**9**][CF_3SO_3]$_8$: Yield: 315 mg (83%). ν_{max}/cm^{-1} 3070 (m, aromatic, C–H), 1528 (s, dobq, C=O), 1260 (s, triflate, C–F), 1217 (s, porphyrin, N–H). λ_{max}/nm ($\varepsilon/M^{-1}\,cm^{-1}$) ($1.0 \times 10^{-5}$ M, CH_2Cl_2) 413 (3.49×10^5), 519 (0.54×10^5). δ_H (400 MHz, CD_3CN, 298 K) 8.99 (m, 8H, H_{pyr}), 8.90 (d, ^3J 7.2, 8H, H'_α), 8.82 (m, 16H, $H_\beta + H_\alpha$), 8.29 (m, 8H, H'_{pyr}), 7.43 (d, ^3J 7.4, 8H, H'_β), 6.33 (d, ^3J 6.3, 8H, H_{indane}), 6.25 (d, ^3J 6.2, 8H, H_{indane}), 6.15 (s, 8H, H_q), 6.08 (t, 8H, H_{indane}), 6.02 (t, 8H, H_{indane}), 3.06 (m, 16H, $CH_{2indane}$), 2.95 (m, 8H, $CH_{2indane}$), −6.96 (s, 4H, NH). $^{13}C\{^1H\}$ NMR (100 MHz, CD_3CN, 298 K) 184.9 (CO), 184.8 (CO), 153.5 (CH'_α), 152.2 (CH_α), 151.7 ($C_{pyridyl}$), 133.7 (C_{pyr}), 133.5 (C_{pyr}), 132.5 (CH'_β), 132.0 (CH_β), 127.0 (CH'_{pyr}), 126.9 (CH'_{pyr}), 105.1 (C_{indane}), 104.8 (C_{indane}), 102.9 (CH_q), 83.2 (CH_{indane}), 83.0 (CH_{indane}), 82.8 (CH_{indane}), 82.7 (CH_{indane}), 30.7 ($CH_{2indane}$), 23.5 ($CH_{2indane}$). *m/z* (ESI) 1035.5 $[\mathbf{9} + (CF_3SO_3)_4]^{4+}$. Calc. for $C_{184}H_{140}F_{24}N_{16}O_{40}Ru_8S_8$ (4736.2): C 46.66, H 2.98, N 4.73. Found: C 46.44, H 2.92, N 4.58%.

[**10**][CF_3SO_3]$_8$: Yield: 337 mg (78%). ν_{max}/cm^{-1} 3068 (m, aromatic, C–H), 1522 (s, dobq, C=O), 1259 (s, triflate, C–F), 1220 (s, porphyrin, N–H). λ_{max}/nm ($\varepsilon/M^{-1}\,cm^{-1}$) ($1.0 \times 10^{-5}$ M, CH_2Cl_2) 412 (4.05×10^5), 522 (0.69×10^5). δ_H (400 MHz, CD_3CN, 298 K) 8.90 (d, ^3J 6.5, 8H, H_{pyr}), 8.84 (d, ^3J 7.2, 8H, H'_α), 8.63 (m, 16H, $H_\beta + H_\alpha$), 8.30 (d, 8H, H'_{pyr}), 7.42 (d, ^3J 7.4, 8H, H'_β), 6.33 (dd, ^3J 5.6, ^3J 6.0, 16H, H_{phenyl}), 6.25 (s, 8H, H_q), 6.15 (t, ^3J 5.6, 8H, H_{phenyl}), 6.09 (dd, ^3J 5.6, ^3J 6.0, 8H, H_{phenyl}), 6.02 (d, ^3J 6.0, 8H, H_{phenyl}), 2.77 (t, ^3J 7.8, 16H, $CH_{2\alpha}$), 1.52 (m, 16H, $CH_{2\beta}$), 1.33 (m, 96H, CH_2), 0.89 (m, 24H, CH_3), −6.96 (s, 4H, NH). $^{13}C\{^1H\}$ NMR (100 MHz, CD_3CN, 298 K)

185.2 (CO), 184.8 (CO), 153.5 (CH'_{α}), 152.5 (CH_{α}), 152.2 ($C_{pyridyl}$), 132.9 (C_{pyr}), 132.7 (C_{pyr}), 132.6 (CH'_{β}), 129.3 (CH_{β}), 129.2 (CH'_{pyr}), 123.8 (CH'_{pyr}), 108.5 (C_q), 102.8 (CH_q), 90.1 (C_{phenyl}), 89.8 (C_{phenyl}), 80.4 (CH_{phenyl}), 79.9 (CH_{phenyl}), 78.4 (CH_{phenyl}), 33.8 ($CH_{2\alpha}$), 32.6 ($CH_{2\beta}$), 30.2 (CH_2), 30.0 (CH_2), 29.9 (CH_2), 23.4 (CH_2), 14.4 (CH_3). *m/z* (ESI) 1207.8 $[\mathbf{10} + (CF_3SO_3)_4]^{4+}$. Calc. for $C_{232}H_{252}F_{24}N_{16}O_{40}Ru_8S_8$ (5425.6): C 51.36, H 4.68, N 4.13. Found: C 51.10, H 4.61, N 4.02%.

Cell Culture and Inhibition of Cell Growth

Human A2780 and A2780cisR ovarian carcinoma cells were obtained from the European Centre of Cell Cultures (ECACC, Salisbury, UK) and maintained in culture as described by the provider. The cells were routinely grown in RPMI 1640 medium with GlutaMAX^{TM} containing 10% fetal calf serum (FCS) and antibiotics (penicillin and ciproxin) at 37°C and 5% CO_2. For the evaluation of growth inhibition, the cells were seeded in 96-well plates and grown for 24 h in complete medium. Complexes were added to the required concentration and added to the cell culture for 72 h incubation. Solutions of the compounds were applied by diluting a freshly prepared stock solution of the corresponding compound in aqueous RPMI medium with GlutaMAX (20 mM). The MTT (thiazolyl blue tetrazolium bromide) test was performed in the last 2 h of the experiment without changing the culture medium. Following drug exposure, MTT was added to the cells at a final concentration of 0.25 mg mL^{-1} and incubated for 2 h, then the culture medium was aspirated and the violet formazan (artificial chromogenic precipitate of the reduction of tetrazolium salts by dehydrogenases and reductases) dissolved in DMSO. The optical density of each well (96-well plates) was quantified three times in triplicates at 540 nm using a multiwell plate reader (iEMS Reader MF, Labsystems, US), and the percentage of surviving cells was calculated from the ratio of absorbance of treated to untreated cells. The IC_{50} values for the inhibition of cell growth were determined by fitting the plot of the logarithmic percentage of surviving cells against the logarithm of the drug concentration using a linear regression function. The median value and the median absolute deviation were obtained from *Excel* software (Microsoft) and those values are reported in Table 1.

References

[1] Y. Matsumura, H. Maeda, *Cancer Res.* **1986**, *46*, 6387.

[2] H. Maeda, *Adv. Enzyme Regul.* **2001**, *41*, 189. doi:10.1016/S0065-2571(00)00013-3

[3] (a) D. F. Baban, L. W. Seymour, *Adv. Drug Deliv. Rev.* **1998**, *34*, 109. doi:10.1016/S0169-409X(98)00003-9
(b) S. Modi, J. P. Jain, A. J. Domb, N. Kumar, *Curr. Pharm. Des.* **2006**, *12*, 4785. doi:10.2174/138161206779026272

[4] (a) M. Galanski, M. A. Jakupec, B. K. Keppler, *Curr. Med. Chem.* **2005**, *12*, 2075. doi:10.2174/0929867054637626
(b) P. Heffeter, U. Jungwirth, M. Jakupec, C. Hartinger, M. Galanski, L. Elbling, M. Micksche, B. Keppler, W. Berger, *Drug Res. Upd.* **2008**, *11*, 1. doi:10.1016/J.DRUP.2008.02.002

[5] A. Warnecke, I. Fichtner, D. Garmann, U. Jaehde, F. Kratz, *Bioconjug. Chem.* **2004**, *15*, 1349. doi:10.1021/BC049829J

[6] (a) A. Levina, A. Mitra, P. A. Lay, *Metallomics* **2009**, *1*, 458. doi:10.1039/B904071D
(b) W. H. Ang, P. J. Dyson, *Eur. J. Inorg. Chem.* **2006**, 4003. doi:10.1002/EJIC.200600723

[7] (a) J. M. Rademaker-Lakhai, D. Van den Bongard, D. Pluim, J. H. Beijnen, J. H. M. Schellens, *Clin. Cancer Res.* **2004**, *10*, 3717. doi:10.1158/1078-0432.CCR-03-0746
(b) C. G. Hartinger, S. Zorbas-Seifried, M. A. Jakupec, B. Kynast, H. Zorbas, B. K. Keppler, *J. Inorg. Biochem.* **2006**, *100*, 891. doi:10.1016/J.JINORGBIO.2006.02.013
(c) C. G. Hartinger, M. A. Jakupec, S. Zorbas-Seifried, M. Groessl, A. Egger, W. Berger, H. Zorbas, P. J. Dyson, B. K. Keppler, *Chem. Biodivers.* **2008**, *5*, 2140. doi:10.1002/CBDV.200890195

[8] (a) A. R. Timerbaev, C. G. Hartinger, S. S. Aleksenko, B. K. Keppler, *Chem. Rev.* **2006**, *106*, 2224. doi:10.1021/CR040704H
(b) W. H. Ang, E. Daldini, L. Juillerat-Jeanneret, P. J. Dyson, *Inorg. Chem.* **2007**, *46*, 9048. doi:10.1021/IC701474M
(c) M. Groessl, E. Reisner, C. G. Hartinger, R. Eichinger, O. Semenova, A. R. Timerbaev, M. A. Jakupec, V. B. Arion, B. K. Keppler, *J. Med. Chem.* **2007**, *50*, 2185. doi:10.1021/JM061081Y
(d) M. Groessl, C. G. Hartinger, K. Polec-Pawlak, M. Jarosz, B. K. Keppler, *Electrophoresis* **2008**, *29*, 2224. doi:10.1002/ELPS.200780790
(e) W. Hu, Q. Luo, X. Ma, K. Wu, J. Liu, Y. Chen, S. Xiong, J. Wang, P. J. Sadler, F. Wang, *Chemistry* **2009**, *15*, 6586. doi:10.1002/CHEM.200900699
(f) O. Nováková, A. A. Nazarov, C. G. Hartinger, B. K. Keppler, V. Brabec, *Biochem. Pharmacol.* **2009**, *77*, 364. doi:10.1016/J.BCP.2008.10.021
(g) M. Gras, B. Therrien, G. Süss-Fink, A. Casini, F. Edafe, P. J. Dyson, *J. Organomet. Chem.* **2010**, *695*, 1119. doi:10.1016/J.JORGANCHEM.2010.01.020
(h) M. Groessl, Y. O. Tsybin, C. G. Hartinger, B. K. Keppler, P. J. Dyson, *J. Biol. Inorg. Chem.* **2010**, *15*, 677. doi:10.1007/S00775-010-0635-0

[9] (a) A. F. A. Peacock, P. J. Sadler, *Chem. Asian J.* **2008**, *3*, 1890. doi:10.1002/ASIA.200800149
(b) C. G. Hartinger, P. J. Dyson, *Chem. Soc. Rev.* **2009**, *38*, 391. doi:10.1039/B707077M
(c) P. J. Dyson, *Chimia* **2007**, *61*, 698. doi:10.2533/CHIMIA.2007.698
(d) G. Süss-Fink, *Dalton Trans.* **2010**, 1673. doi:10.1039/B916860P

[10] J. Mattsson, P. Govindaswamy, A. K. Renfrew, P. J. Dyson, P. Štěpnička, G. Süss-Fink, B. Therrien, *Organometallics* **2009**, *28*, 4350. doi:10.1021/OM900359J

[11] (a) M. G. Mendoza-Ferri, C. G. Hartinger, R. E. Eichinger, N. Stolyarova, K. Severin, M. A. Jakupec, A. A. Nazarov, B. K. Keppler, *Organometallics* **2008**, *27*, 2405. doi:10.1021/OM800207T
(b) M. G. Mendoza-Ferri, C. G. Hartinger, M. A. Mendoza, M. Groessl, A. E. Egger, R. E. Eichinger, J. B. Mangrum, N. P. Farrell, M. Maruszak, P. J. Bednarski, F. Klein, M. A. Jakupec, A. A. Nazarov, K. Severin, B. K. Keppler, *J. Med. Chem.* **2009**, *52*, 916. doi:10.1021/JM8013234
(c) O. Nováková, A. A. Nazarov, C. G. Hartinger, B. K. Keppler, V. Brabec, *Biochem. Pharmacol.* **2009**, *77*, 364. doi:10.1016/J.BCP.2008.10.021

[12] B. Therrien, G. Süss-Fink, P. Govindaswamy, A. K. Renfrew, P. J. Dyson, *Angew. Chem. Int. Ed.* **2008**, *47*, 3773. doi:10.1002/ANIE.200800186

[13] O. Zava, J. Mattsson, B. Therrien, P. J. Dyson, *Chemistry* **2010**, *16*, 1428. doi:10.1002/CHEM.200903216

[14] Y.-F. Han, Y.-J. Lin, L.-H. Weng, H. Berke, G.-X. Jin, *Chem. Commun.* **2008**, 350. doi:10.1039/B711809K

[15] (a) N. P. E. Barry, M. Austeri, J. Lacour, B. Therrien, *Organometallics* **2009**, *28*, 4894. doi:10.1021/OM900461S
(b) N. P. E. Barry, N. H. Abd Karim, R. Vilar, B. Therrien, *Dalton Trans.* **2009**, 10717. doi:10.1039/B913642H

[16] N. P. E. Barry, P. Govindaswamy, J. Furrer, G. Süss-Fink, B. Therrien, *Inorg. Chem. Commun.* **2008**, *11*, 1300. doi:10.1016/J.INOCHE.2008.08.007

[17] (a) P. Govindaswamy, D. Linder, J. Lacour, G. Süss-Fink, B. Therrien, *Chem. Commun.* **2006**, 4691. doi:10.1039/B610155K
(b) P. Govindaswamy, D. Linder, J. Lacour, G. Süss-Fink, B. Therrien, *Dalton Trans.* **2007**, 4457. doi:10.1039/B709247D

(c) B. Therrien, G. Süss-Fink, *Chimia* **2008**, *62*, 514. doi:10.2533/CHIMIA.2008.514

[18] L. L. Gladkov, K. N. Solovyov, *Spectrochim. Acta (A)* **1986**, *42*, 1. doi:10.1016/0584-8539(86)80122-2

[19] X.-Y. Li, R. S. Czernuszewicz, J. R. Kincaid, P. Stein, T. G. Spiro, *J. Phys. Chem.* **1990**, *94*, 47. doi:10.1021/J100364A008

[20] H. Yan, G. Süss-Fink, A. Neels, H. Stoeckli-Evans, *J. Chem. Soc., Dalton Trans.* **1997**, 4345. doi:10.1039/A704658H

[21] (a) F. Ricchelli, *J. Photochem. Photobiol. B* **1995**, *29*, 109. doi:10.1016/1011-1344(95)07155-U
(b) N. P. E. Barry, O. Zava, J. Furrer, P. J. Dyson, B. Therrien, *Dalton Trans.* **2010**, 5272. doi:10.1039/C001521K

[22] (a) R. A. Zelonka, M. C. Baird, *Can. J. Chem.* **1972**, *50*, 3063. doi:10.1139/V72-486
(b) M. A. Bennett, T.-N. Huang, T. W. Matheson, A. K. Smith, *Inorg. Synth.* **1982**, *21*, 74. doi:10.1002/9780470132524.CH16

[23] L. Vieille-Petit, B. Therrien, G. Süss-Fink, *Acta Crystallogr.* **2002**, *E58*, m656. doi:10.1107/S1600536802018676

[24] P. S. Engel, R. L. Allgren, W.-K. Chae, R. A. Leckonby, N. A. Marron, *J. Org. Chem.* **1979**, *44*, 4233. doi:10.1021/JO01338A004

[25] B. Therrien, *Coord. Chem. Rev.* **2009**, *253*, 493. doi:10.1016/J.CCR.2008.04.014